

# Wideband Tunable Differential Phase Shifter With Minimized In-Band Phase Deviation Error

Girdhari Chaudhary<sup>id</sup>, *Member, IEEE*, and Yongchae Jeong<sup>id</sup>, *Senior Member, IEEE*

**Abstract**—This letter presents a tunable differential phase shifter with wideband flat phase characteristics. The proposed structure consists of a power dividing circuit and two 3-dB hybrids. To achieve the tunable flat phase characteristics over a wide bandwidth (BW), the coupled and through ports of one hybrid is terminated with short-circuited transmission lines (TLs), whereas those of another hybrid are terminated with a TL and varactor diode. For experimental validation, the proposed structure was designed and fabricated at a center frequency of 2.5 GHz. From the measurement results, the fabricated circuit provided a tunable differential phase shift range of 89° to 193° with a maximum in-band phase error of ±8.6° over a BW of 1 GHz.

**Index Terms**—Phase slope adjustment, tunable differential phase shifter, varactor diode, wideband flat phase.

## I. INTRODUCTION

TUNABLE phase shifters with flat magnitude and phase characteristics are highly demanded for phased-array antennas, beamforming networks, antenna feeding network, and robust signal interference cancellation in full duplex antennas [1], [2]. Over the past decades, various nonreconfigurable differential phase shifters have been studied using different technologies [3]–[7]. The Schiffman phase shifter, which consists of shorted edge-coupled line as main line and a uniform transmission line (TL) in the reference line, is reported in [3]. Wideband differential phase shifters are demonstrated by adjusting the phase slopes of multimode resonators, three coupled lines, and stubs in [4]–[6]. Similarly, the differential phase shifters integrated with a filtering function was proposed in [7]. However, these reported structures cannot provide tunable differential phase characteristics.

Several tunable phase shifters have been reported [8]–[12]. However, these structures have a high in-band phase deviation error within the operating bandwidth (BW) when these circuits are utilized to operate as differential phase shifters with respect to the reference line [8]–[11]. In fact, the design of tunable differential phase shifter with flat magnitude and

Manuscript received May 7, 2019; revised May 24, 2019; accepted May 28, 2019. Date of publication June 19, 2019; date of current version July 3, 2019. This work was supported in part by the Korean Research Fellowship Program through the National Research Foundation (NRF) of Korea funded by the Ministry of Science and ICT under Grant 2016H1D3A1938065, in part by the Basic Science Research Program through the National Research Foundation of Korea (NRF) funded by Ministry of Education, Science and Technology under Grant 2016R1D1A1B03931400, and in part by Basic Science Research Program through NRF funded by Ministry of Education under Grant 2019R1A6A1A09031717 (Corresponding author: Yongchae Jeong.)

The authors are with the Division of Electronics and Information Engineering, IT Research Center, Chonbuk National University, Jeonju 54896, South Korea (e-mail: girdharic@jbnu.ac.kr; ycjeong@jbnu.ac.kr).

Color versions of one or more of the figures in this paper are available online at <http://ieeexplore.ieee.org>.

Digital Object Identifier 10.1109/LMWC.2019.2920270

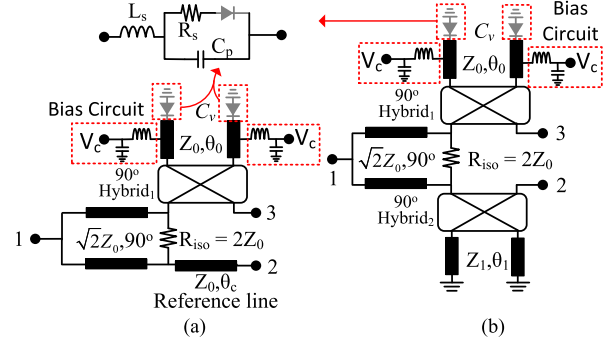


Fig. 1. Structures of tunable differential phase shifter. (a) Conventional one (b) Proposed.

phase characteristics (low in-band differential phase deviation error) is challenging research. In [11], a differential tunable shifter is demonstrated without the experimental results using a distributed loaded TL and coupled line.

In this letter, we demonstrate a wideband differential tunable phase shifter with flat phase and magnitude characteristics. To achieve the flat differential tunable phase characteristics, the phase slopes of the different transmission paths are maintained the same. To achieve consistent simulation results with measurement, frequency-dependent capacitance of varactor extracted from the equivalent circuit model provided by manufacture has been utilized to obtain optimum circuit parameters of the proposed structure.

## II. THEORY AND DESIGN EQUATIONS

Fig. 1 shows the structures of the tunable differential phase shifter. In the proposed structure, the coupled and through ports of one 3-dB hybrid were terminated with a TL ( $Z_0, \theta_0$ ) and varactor diode ( $C_v$ ), whereas those of other hybrids are terminated with a short-circuited TL ( $Z_1, \theta_1$ ) for achieving flat phase characteristics. For mathematical simplicity, the capacitance of the varactor diode is assumed as  $C_v$ . Since the structure is not symmetrical, the modified even- and odd-mode analysis should be used where signal transmission occurs under the modified even-mode excitation only. Assuming both the 3-dB hybrids are identical and perfect, the phase difference between the input port ① and output ports (port ② and ③) can be expressed as

$$\Delta\varphi = \varphi_A - \varphi_B \quad (1)$$

where

$$\varphi_A = 2 \tan^{-1} \left\{ 2\pi f C_v Z_0 \tan \frac{\theta_0 f}{f_0} - 1 / \tan \frac{\theta_0 f}{f_0} + 2\pi f Z_0 C_v \right\} \quad (2a)$$

$$\varphi_B = 2 \tan^{-1} \{ Z_1 / Z_0 \tan(\theta_1 f / f_0) \} \quad (2b)$$

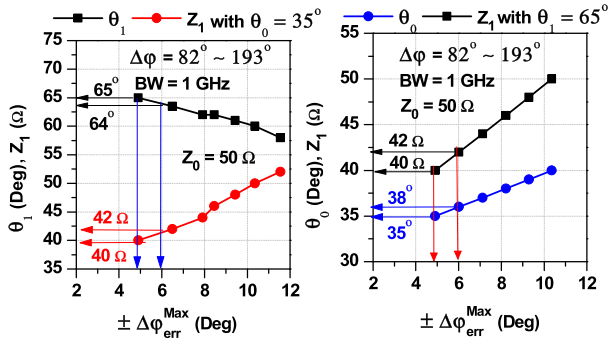


Fig. 2. Calculated circuit parameter values of proposed tunable differential phase shifter using equivalent circuit model of varactor SMV-1231 (parasitic components:  $L_s = 0.7689$  nH,  $R_s = 1.5$   $\Omega$ , and  $C_p = 0.27$  pF) for operating BW of 1 GHz at  $f_0 = 2.50$  GHz.

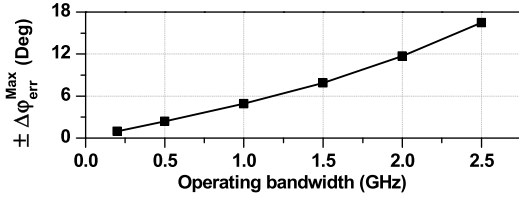


Fig. 3. Maximum in-band differential phase deviation errors according to operating BW.

and  $Z_0$ ,  $f$ , and  $f_0$  are port impedance, operating frequency, and design center frequency, respectively.

To achieve the flat  $\Delta\phi$ , the phase slopes (incremental rate of phase) between ports ②, ① and ports ③, ① should be the same. Finally, the in-band differential phase error ( $\Delta\phi_{\text{err}}$ ) within the operating BW can be defined as follows:

$$\Delta\phi_{\text{err}} = \frac{\pm(\Delta\phi_{\text{max}} - \Delta\phi_{\text{min}})}{2} \quad (3)$$

The varactor diode has parasitic components as well as frequency-dependent capacitance, which can deteriorate the differential phase flatness. Therefore, the equivalent circuit model of the varactor diode shown in Fig. 1 provided by the manufacturer should be used to obtain optimum circuit parameters for flat phase characteristics within the operating BW. In this letter, varactor SMV-1231 from Skyworks with parasitic components  $L_s = 0.7689$  nH,  $R_s = 1.5$   $\Omega$ , and  $C_p = 0.27$  pF is used.  $C_v$  is varied from 0.42 to 4.17 pF at  $f_0 = 2.5$  GHz when the bias voltage was applied from 18 to 0 V. After obtaining frequency-dependent  $C_v$ , the circuit parameters of the proposed circuit with given specifications (such as  $f_0$ , BW,  $\Delta\phi$  tunable range, and maximum allowed error  $\Delta\phi_{\text{ref\_err}}$ ) can be estimated using (1)–(3) in MATLAB.

For the design graphs, Fig. 2 shows the calculated circuit parameter values of the proposed tunable differential phase shifter. In this calculation, the extracted  $C_v$  from an equivalent model of the varactor diode SMV-1231 was used to make simulation results consistent with the measurement. Similarly, a tunable range of  $\Delta\phi$  ( $\Delta\phi_{\text{lower}} \sim \Delta\phi_{\text{upper}}$ ) is maintained for  $82^\circ$  to  $193^\circ$  within an operating BW of 1 GHz. As shown in Fig. 2,  $\Delta\phi_{\text{err}}$  is increased with the increase of  $Z_1$  and decrease of  $\theta_1$ . In the case of the fixed  $\theta_1$ ,  $\Delta\phi_{\text{err}}$  is increased when  $\theta_0$  and  $Z_1$  increase. Fig. 3 shows the maximum  $\Delta\phi_{\text{err}}$  with operating BWs. From this figure, it is concluded that

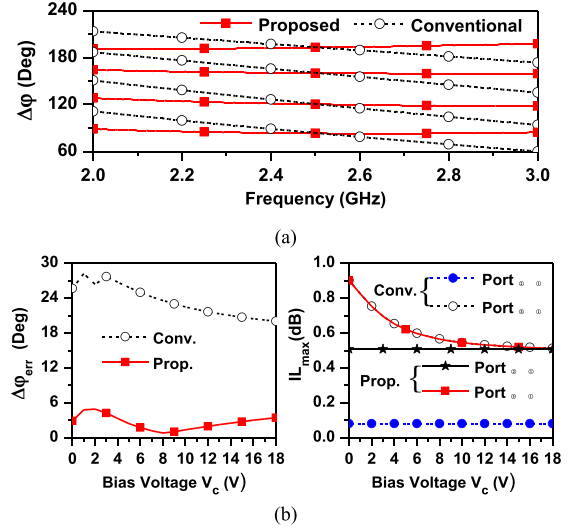


Fig. 4. Simulated results of differential phase shifters using varactor SMV-1231 and circuit parameters.  $Z_1 = 40$   $\Omega$ ,  $\theta_1 = 65^\circ$ ,  $Z_0 = 50$   $\Omega$ ,  $\theta_0 = 35^\circ$ , and  $\theta_c = 30^\circ$  and assuming 0.2-dB IL of 3-dB hybrids. (a) Differential phase shift (b) In-band phase deviation error/IL.

operating BW can be enhanced if higher  $\Delta\phi_{\text{err}}$  is acceptable for application.

To validate the analytical analysis, Fig. 4 shows the simulation results of the conventional and proposed tunable differential phase shifters using equivalent circuit model of the varactor SMV-1231 from Skyworks. As shown in Fig. 4, the proposed tunable differential phase shifter provides flat phase characteristics with a maximum  $\Delta\phi_{\text{err}}$  of  $\pm 4.90^\circ$  for  $\Delta\phi = 82^\circ$ – $193^\circ$ , whereas the conventional structure has maximum phase error of  $\pm 28.16^\circ$  for the same  $\Delta\phi$  range. Similarly, the insertion loss (IL) between ports ③ and ① of the proposed circuit is similar to the conventional one. Although the IL between ports ② and ① is slightly higher than the conventional one, the differential phase characteristics are much flatter, as well as magnitude imbalance is small over the wide BW.

### III. IMPLEMENTATION AND EXPERIMENTAL PERFORMANCES

For experimental demonstration, the circuit was designed for the operating BW of 1 GHz at  $f_0 = 2.5$  GHz. The design goal was to achieve  $\Delta\phi$  ( $\Delta\phi_{\text{lower}} \sim \Delta\phi_{\text{upper}}$ ) =  $90^\circ$ – $195^\circ$  and a maximum  $\Delta\phi_{\text{ref\_err}}$  of  $\pm 5^\circ$ . Based on the above design specification, the circuit parameters are obtained using MATLAB (see Fig. 3) as  $Z_1 = 40$   $\Omega$ ,  $\theta_1 = 65^\circ$ ,  $Z_0 = 50$   $\Omega$ ,  $\theta_0 = 35^\circ$ , and  $C_v = 0.45$ – $4.16$  pF at  $f_0$ . The prototype circuit was fabricated using substrate RT/Duroid 5880 ( $\epsilon_r = 2.2$  and  $h = 0.787$  mm). Similarly, 3-dB  $90^\circ$  hybrids S03A2500N1 from ANAREN were used in this letter because of their wideband characteristics. The amplitude and phase errors of the 3-dB hybrids between the through and coupling ports were within  $\pm 0.4$  dB and  $90 \pm 2^\circ$  for 2–3 GHz.

Fig. 5 shows the simulation and measurement results of the fabricated prototype. The measurement results were consistent with the simulations. From the experiment, the  $\Delta\phi$  is tuned from  $88^\circ$  to  $193^\circ$  with a maximum  $\Delta\phi_{\text{err}}$  of  $\pm 8.6^\circ$  and maximum IL of 1.06 dB for the operating BW of 1 GHz

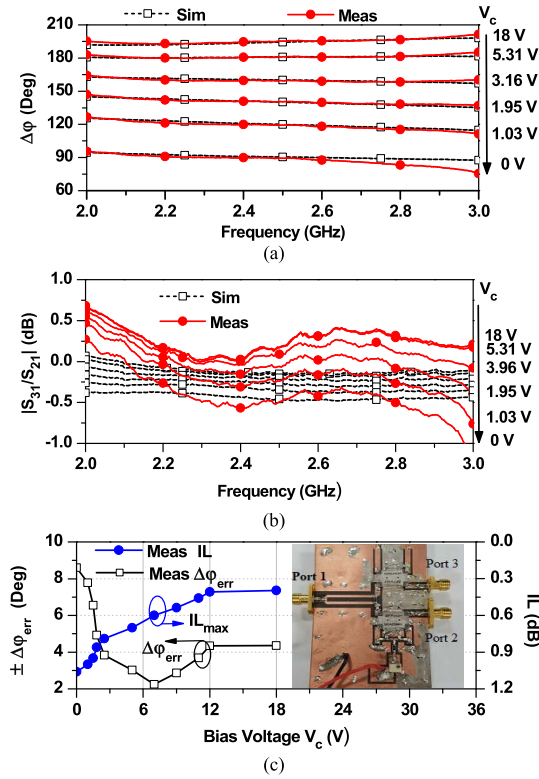


Fig. 5. Simulated and measured results for proposed tunable differential phase shifter. (a) Phase difference. (b) Magnitude difference. (c) In-band phase deviation error.

TABLE I  
PERFORMANCE COMPARISON WITH THE STATE OF THE ART

	$f_0$ (GHz)	BW (GHz)	$\Delta\phi_{\max}$ ( $^\circ$ )	$\Delta\phi_{\text{err}}^{\max}$ ( $^\circ$ )	$\text{IL}_{\max}$ (dB)	$\text{RL}_{\min}$ (dB)	A (Y/N)	FoM
[3]	2.3	1.2	90	$\pm 2$	1	12	N	NA
[4]	3	1.41	180	$\pm 3.4$	x	12.5	N	NA
[5]	3	3.07	135	$\pm 5$	x	10	N	NA
[6]	2	1.67	180	$\pm 4$	0.5	15	N	NA
[7]	3	0.62	180	$\pm 4.20$	2.2	13	N	NA
[8]	2	0.2	385	$\pm 55$	1	11	Y	2.21
[9]	2	0.2	234	$\pm 45$	4.6	13	Y	1.37
[10]	2.2	0.9	372.5	$\pm 21$	3.20	7.8	Y	11.11
[11]	1	1	28*	$\pm 8$	5	5	Y	3.50
[12]	2.5	0.5	146.9	$\pm 5.8$	1.28	15.76	Y	26.87
<b>This work</b>	<b>2.5</b>	<b>1</b>	<b>104</b>	<b><math>\pm 8.6</math></b>	<b>1.06</b>	<b>16.5</b>	<b>Y</b>	<b>28.62</b>

A: Reconfigurable phase characteristics, Y : Yes, N: No  
\*: EM simulation results.

at  $f_0 = 2.5$  GHz. Similarly, the measured input–output return loss (RL) and isolation between the output ports were higher than 16.5 and 37.7 dB at  $f_0 = 2.50$  GHz for overall tunable differential phase range, respectively.

A tunable differential phase shifter should provide a high  $\Delta\phi$  tuning range, low  $\Delta\phi_{\text{err}}$ , low IL, and high RL within a wide operating BW. To compare the performances with the state of the art, the figure of merit (FoM) is defined as (4) by considering these requirements

$$\text{FoM} = \frac{\text{BW}(\text{GHz}) \times \Delta\phi_{\max}(\text{rad})}{f_0(\text{GHz}) \times \Delta\phi_{\text{err}}^{\max}(\text{rad})} \times \frac{10^{\left(\frac{-\text{IL}_{\max}(\text{dB})}{20}\right)}}{10^{\left(\frac{-\text{RL}_{\min}(\text{dB})}{20}\right)}}. \quad (4)$$

As can be observed in Table I, [3]–[7] provide a fixed differential phase difference  $\Delta\phi$ , with a small phase error  $\Delta\phi_{\text{err}}$ , over wide BW. Because of the nontunable  $\Delta\phi$  characteristics of these works, the FoMs are not listed in Table I. Configurations in [8]–[11] can provide a large tunable  $\Delta\phi$  range with respect to the reference line [see Fig. 1(a)]. However,  $\Delta\phi_{\text{err}}$  is high within the operating BW. Conversely, this letter exhibits the highest FoM as compared to the state of the art as well as tunable  $\Delta\phi$  with a small  $\Delta\phi_{\text{err}}$  over a wide operating BW.

#### IV. CONCLUSION

In this letter, we demonstrated a wideband tunable differential phase shifter with a very low in-band phase deviation error using hybrids. To achieve flat differential phase characteristics over the wideband, the phase slopes (incremental rate of phase) between two transmission paths were maintained the same by terminating the through and coupled ports of one hybrid with short-circuited TLs and those of other hybrids with varactor diode and TL. Both theoretical and experimental results are provided for validation of structure. Since the proposed structure provides flat tunable differential phase characteristics, it is promising for the phase-array antennas as well as robust self-interference cancellation application in the in-band full duplex system.

#### REFERENCES

- [1] C.-C. Chang, R.-H. Lee, and T.-Y. Shih, "Design of a beam switching/steering butler matrix for phased array system," *IEEE Trans. Antennas Propag.*, vol. 58, no. 2, pp. 367–374, Feb. 2010.
- [2] S. Khaledian, F. Farzami, B. Smida, and D. Erricolar, "Robust self-interference cancellation for microstrip antennas by means of phase reconfigurable coupler," *IEEE Trans. Antennas Propag.*, vol. 66, no. 10, pp. 5574–5579, Oct. 2018.
- [3] Y.-X. Guo, Z.-Y. Zhang, and L. C. Ong, "Improved wide-band Schiffman phase shifter," *IEEE Trans. Microw. Theory Techn.*, vol. 54, no. 3, pp. 1196–1200, Mar. 2006.
- [4] Y.-P. Lyu, L. Zhu, Q.-S. Wu, and C.-H. Cheng, "Proposal and synthesis design of wideband phase shifters on the multimode resonator," *IEEE Trans. Microw. Theory Techn.*, vol. 64, no. 12, pp. 4211–4221, Dec. 2016.
- [5] X. Yu, S. Sun, X. Jing, and L. Zhu, "Design of ultraflat phase shifters using multiple quarter-wavelength short-ended stubs," *IEEE Microw. Wireless Compon. Lett.*, vol. 29, no. 4, pp. 246–248, Apr. 2019.
- [6] H.-J. Yoon and B.-W. Min, "Wideband 180° phase shifter using parallel-coupled three-line," *IEEE Microw. Wireless Compon. Lett.*, vol. 29, no. 2, pp. 89–91, Feb. 2019.
- [7] Y.-P. Lyu, L. Zhu, and C.-H. Cheng, "Proposal and synthesis design of differential phase shifters with filtering function," *IEEE Trans. Microw. Theory Techn.*, vol. 65, no. 8, pp. 2906–2917, Aug. 2017.
- [8] F. Burdin, Z. Iskandar, F. Podevin, and P. Ferrari, "Design of compact reflection-type phase shifters with high figure-of-merit," *IEEE Trans. Microw. Theory Techn.*, vol. 63, no. 6, pp. 1883–1893, Jun. 2015.
- [9] C.-S. Lin, S.-F. Chang, C.-C. Chang, and Y.-H. Shu, "Design of a reflection-type phase shifter with wide relative phase shift and constant insertion loss," *IEEE Trans. Microw. Theory Techn.*, vol. 55, no. 9, pp. 1862–1868, Sep. 2007.
- [10] A. M. Abbosh, "Compact tunable reflection phase shifters using short section of coupled lines," *IEEE Trans. Microw. Theory Techn.*, vol. 60, no. 8, pp. 2465–2472, Aug. 2012.
- [11] M. Ould-Elhassen, M. Mabrouk, A. Ghazel, and P. Benech, "Differential tunable phase shifter," in *Proc. IEEE Int. Symp. Phased Array Syst. Technol.*, Oct. 2013, pp. 97–101.
- [12] B. An, G. Chaudhary, and Y. Jeong, "Wideband tunable phase shifter with low in-band phase deviation using coupled line," *IEEE Microw. Wireless Compon. Lett.*, vol. 28, no. 5, pp. 678–680, Aug. 2018.